

AN ADAPTIVE FRAMEWORK FOR FIRST-ORDER GRADIENT METHODS*

XIAOZHE HU[†], SARA POLLOCK[‡], ZHONGQIN XUE[†], AND YUNRONG ZHU[§]

Abstract. Gradient methods are widely used in optimization problems. In practice, while the smoothness parameter can be estimated utilizing techniques such as backtracking, estimating the strong convexity parameter remains a challenge; moreover, even with the optimal parameter choice, convergence can be slow. In this work, we propose a framework for dynamically adapting the step size and momentum parameters in first-order gradient methods for the optimization problem, without prior knowledge of the strong convexity parameter. The main idea is to use the geometric average of the ratios of successive residual norms as an empirical estimate of the upper bound on the convergence rate, which in turn allows us to adaptively update the algorithm parameters. The resulting algorithms are simple to implement, yet efficient in practice, requiring only a few additional computations on existing information. The proposed adaptive gradient methods are shown to converge at least as fast as gradient descent for quadratic optimization problems. Numerical experiments on both quadratic and nonlinear problems validate the effectiveness of the proposed adaptive algorithms. The results show that the adaptive algorithms are comparable to their counterparts using optimal parameters, and in some cases, they capture local information and exhibit improved performance.

Key words. gradient methods, strongly convex, quadratic optimization, adaptive algorithm

MSC codes. 65K05, 65K10, 68Q25, 90C25

1. Introduction. Many problems in machine learning [9, 35, 3], signal processing [21, 27], and operations research [22, 28] are formulated as optimization problems:

$$\min_{\mathbf{x} \in \mathbb{R}^n} f(\mathbf{x}),$$

where we assume that $f : \mathbb{R}^n \rightarrow \mathbb{R}$ is a differentiable function. The function f is said to be L -smooth if its gradient is Lipschitz continuous with constant $L > 0$, that is,

$$\|\nabla f(\mathbf{x}) - \nabla f(\mathbf{y})\| \leq L\|\mathbf{x} - \mathbf{y}\|, \quad \forall \mathbf{x}, \mathbf{y} \in \mathbb{R}^n.$$

The function f is convex if it satisfies

$$f(\mathbf{y}) \geq f(\mathbf{x}) + \langle \nabla f(\mathbf{x}), \mathbf{y} - \mathbf{x} \rangle, \quad \forall \mathbf{x}, \mathbf{y} \in \mathbb{R}^n.$$

Furthermore, f is said to be μ -strongly convex with parameter $\mu > 0$ if

$$f(\mathbf{y}) \geq f(\mathbf{x}) + \langle \nabla f(\mathbf{x}), \mathbf{y} - \mathbf{x} \rangle + \frac{\mu}{2}\|\mathbf{y} - \mathbf{x}\|^2, \quad \forall \mathbf{x}, \mathbf{y} \in \mathbb{R}^n.$$

One of the most commonly used methods for solving such problems is the gradient descent (GD) algorithm. When f is convex and L -smooth, GD achieves a sublinear convergence, which varies with the smoothness of the gradient. For μ -strongly convex problems, the convergence rate of GD improves to linear. However, GD often exhibits

*Submitted to the editors DATE.

Funding: Author SP acknowledges partial support from NSF grant DMS 2045059 (CAREER). The work of XH is partially supported by the National Science Foundation under grant DMS-2513394.

[†]Department of Mathematics, Tufts University, Medford, MA 02155, USA (Xiaozhe.Hu@tufts.edu, Zhongqin.Xue@tufts.edu).

[‡]Department of Mathematics, University of Florida, Gainesville, FL 32611, USA (s.pollock@ufl.edu).

[§]Department of Mathematics and Statistics, Idaho State University, Pocatello, ID 83209, USA (zhuyunr@isu.edu).

slow convergence for ill-conditioned problems. To accelerate convergence, first-order momentum methods were introduced. The Nesterov Accelerated Gradient (NAG) utilizes a “look-ahead” gradient by evaluating ∇f at an extrapolated point achieving an accelerated linear convergence rate compared to GD. By incorporating momentum directly, the heavy-ball (HB) method achieves acceleration for iterations near the minimum of the strongly convex quadratic objective; however, for general strongly convex problems, it may fail to converge [13, 16].

However, in practice, smoothness and strong convexity constants are typically unavailable or costly to obtain in a timely manner during the optimization process. Consequently, much effort has been devoted to designing algorithms that are robust under estimated or unknown parameters. For algorithms with estimated parameters, however, poor estimations may result in slow convergence or even divergence. Backtracking line search methods, originating from the early work of Goldstein [12] and Armijo [1], find a step size along the search direction that ensures sufficient decrease of the objective at each iteration. Nesterov [24] adapts the backtracking idea to estimate the smoothness constant in constructing the accelerated gradient method. On the other hand, restart schemes provide a simple adaptive mechanism that does not require prior knowledge of the problem parameters. Their performance is primarily driven by the choice of restart frequency and the underlying regularity properties. Nesterov [23] designed a restart strategy with linear convergence in the strongly convex setting. Based on the observation that accelerated methods display periodic oscillations when momentum is high, [26] restarts the algorithm when periodic oscillations are detected. There are also some works that investigate restart schemes under the generic Hölderian error bound setting, see [11, 15, 17, 29] for details. Recently, various adaptive strategies are applied to select parameters. Malitsky and Mishchenko [19] develop an adaptive GD algorithm that estimates local smoothness from gradient information. Utilizing primal-dual relations to estimate a local strong convexity constant, they further propose an adaptive accelerated gradient descent algorithm. The authors later extend their approach to construct an adaptive proximal gradient method [20]. Recently, the authors in [34] develop an adaptive NAG that estimates the local smoothness constant via the quadratic upper bound for the L -smooth objective, achieving an $\mathcal{O}(1/k^2)$ convergence rate.

In this work, we illustrate our approach using an unconstrained quadratic optimization problem:

$$(1.1) \quad \min_{\mathbf{x} \in \mathbb{R}^n} f(\mathbf{x}) = \frac{1}{2} \mathbf{x}^T A \mathbf{x} - \mathbf{b}^T \mathbf{x},$$

where $A \in \mathbb{R}^{n \times n}$ is a symmetric positive definite (SPD) matrix and vector $\mathbf{b} \in \mathbb{R}^n$ is given. The function $f(\mathbf{x})$ is strongly convex, smooth and has a unique minimizer \mathbf{x}^* characterized by $\nabla f(\mathbf{x}^*) = 0$, i.e., $A\mathbf{x}^* = \mathbf{b}$. Suppose the eigenvalues of A satisfy $0 < \lambda_1 \leq \dots \leq \lambda_n$. Then the strong convexity and smoothness parameters are given by $\mu = \lambda_1$ and $L = \lambda_n$, respectively, and the condition number is defined as $\kappa := \frac{L}{\mu}$. As discussed above, the smoothness parameter can be estimated via backtracking. Consequently, the main interest of this work is providing a unified framework for developing adaptive methods that do not require prior knowledge of the strong convexity constant μ . To this end, we introduce an adaptive update rule motivated by [2] that uses the geometric average of the ratios of successive residual norms as an empirical estimate of the upper bounds on convergence rates for the first-order gradient methods, which then guides the parameter updates. We prove that the adaptive gradient methods converge at least as fast as GD with a step size

of $1/L$. Numerical results on quadratic problems with diagonal Hessians validate the effectiveness of the proposed adaptive algorithms. We observed that the convergence rate estimate computed from the geometric average of the ratios of successive residual norms asymptotically approaches the optimal convergence rate. Furthermore, the proposed methods, capturing local curvature information, also show good performance on nonlinear problems.

The remainder of this article is organized as follows. In Section 2, we briefly summarize relevant gradient methods and present and analyze the proposed adaptive algorithms. Section 3 reports our numerical results, evaluating the adaptive methods on both quadratic and nonlinear problems. Finally, Section 4 provides concluding remarks and outlines directions for future work.

2. Adaptive Algorithms. In this section, we present adaptive algorithms for solving the quadratic optimization problem (1.1) and investigate their convergence behavior in detail.

To facilitate the discussion, we introduce some standard notation. We use ρ^* as a generic notation for the upper bound on the convergence rate of the gradient methods. The parameters α and β denote the step size and the momentum parameter, respectively. When referring to methods, the corresponding bounds will be denoted by appropriate subscripts. We start with a brief review of three classical first-order algorithms: GD, NAG and HB for quadratic optimization problems in Table 1.

TABLE 1
Classical first-order gradient methods for quadratic optimization problems

Method	Update Rule	Optimal Parameters	Rate Bound
GD	$\mathbf{x}_{k+1} = \mathbf{x}_k - \alpha \nabla f(\mathbf{x}_k)$	$\alpha_{\text{GD}}^* = \frac{2}{L+\mu}$	$\rho_{\text{GD}}^* = \frac{L-\mu}{L+\mu}$
NAG	$\mathbf{y}_k = \mathbf{x}_k + \beta(\mathbf{x}_k - \mathbf{x}_{k-1})$ $\mathbf{x}_{k+1} = \mathbf{y}_k - \alpha \nabla f(\mathbf{y}_k)$	$\alpha_{\text{NAG}}^* = \frac{1}{L}$, $\beta_{\text{NAG}}^* = \frac{\sqrt{L}-\sqrt{\mu}}{\sqrt{L}+\sqrt{\mu}}$	$\rho_{\text{NAG}}^* = 1 - \frac{\sqrt{\mu}}{\sqrt{L}}$
HB	$\mathbf{x}_{k+1} = \mathbf{x}_k - \alpha \nabla f(\mathbf{x}_k)$ $+ \beta(\mathbf{x}_k - \mathbf{x}_{k-1})$	$\alpha_{\text{HB}}^* = \frac{4}{(\sqrt{L}+\sqrt{\mu})^2}$ $\beta_{\text{HB}}^* = \left(\frac{\sqrt{L}-\sqrt{\mu}}{\sqrt{L}+\sqrt{\mu}}\right)^2$	$\rho_{\text{HB}}^* = \frac{\sqrt{L}-\sqrt{\mu}}{\sqrt{L}+\sqrt{\mu}}$

Hereafter, we assume, without loss of generality, that $L \leq 1$. This can be achieved by applying a proper rescaling of A . Specifically, the case $L = 1$ corresponds to knowing the smoothness constant of the objective in the rescaling step. The key idea of the algorithm is to adaptively update the step size α and momentum parameter β based on the information extracted from the observed iterates. In particular, estimates of the convergence rate ρ^* are used to update the parameters based on their relationships outlined in Table 1. We begin by applying this principle to GD and derive an adaptive variant in the next subsection.

2.1. Adaptive Gradient Descent. Define the residual at the k -th iteration as $\mathbf{r}_k := \mathbf{b} - \mathbf{A}\mathbf{x}_k = \mathbf{A}(\mathbf{x}^* - \mathbf{x}_k)$. For GD, the residual sequence satisfies the following recurrence

$$\mathbf{r}_k = (I - \alpha \mathbf{A})\mathbf{r}_{k-1}, \quad k \geq 1.$$

Applying the ℓ^2 norm on both sides, noting that $I - \alpha \mathbf{A}$ is SPD, one arrives at

$$\|\mathbf{r}_k\| \leq \rho(I - \alpha \mathbf{A})\|\mathbf{r}_{k-1}\|,$$

where $\rho(M)$ denotes the spectral radius of a matrix M . When $\alpha = \alpha_{\text{GD}}^*$, we obtain $\rho(I - \alpha A) = \rho_{\text{GD}}^* = \frac{L-\mu}{L+\mu}$. Therefore, we can also rewrite it as

$$(2.1) \quad \mu = L \frac{1 - \rho_{\text{GD}}^*}{1 + \rho_{\text{GD}}^*}.$$

In our adaptive scheme, we simply approximate L as 1. This is justified because estimating the largest eigenvalue is generally computationally inexpensive, allowing us to rescale the system such that $L \approx 1$. The key idea of our proposed adaptive framework is to construct a sequence $\{\rho_k\}$ that serves as an empirical estimate of ρ_{GD}^* at each iteration. Then, (2.1) suggests that we could approximate μ at each iteration by $\mu_k = \frac{1-\rho_k}{1+\rho_k}$, which yields an adaptive step size:

$$\alpha_{\text{GD}}^* = \frac{2}{L + \mu} \implies \alpha_{k+1} = \frac{2}{1 + \mu_k} = 1 + \rho_k.$$

The update rule for the adaptive GD is then given by

$$\mathbf{x}_{k+1} = \mathbf{x}_k - \alpha_{k+1} \nabla f(\mathbf{x}_k).$$

It is summarized in Algorithm 2.1.

Algorithm 2.1 Adaptive Gradient Descent

- 1: **Input:** SPD matrix $A \in \mathbb{R}^{n \times n}$, vector $\mathbf{b} \in \mathbb{R}^n$, initial point $\mathbf{x}_0 \in \mathbb{R}^n$
- 2: **Initialize:** Compute $\mathbf{r}_0 = -\nabla f(\mathbf{x}_0)$, set $\alpha_1 = 1$
- 3: **for** $k = 1, 2, \dots$ **do**
- 4: $\mathbf{x}_k = \mathbf{x}_{k-1} + \alpha_k \mathbf{r}_{k-1}$
- 5: $\mathbf{r}_k = -\nabla f(\mathbf{x}_k)$
- 6: $\rho_k \approx \rho_{\text{GD}}^*$, where ρ_k is an estimate of ρ_{GD}^*
- 7: $\alpha_{k+1} = 1 + \rho_k$
- 8: **end for**

First, we consider the case where the estimate ρ_k is obtained by computing the spectral radius of $I - \alpha_k A$. Note that this case is primarily of theoretical interest, as it is computationally expensive to implement in practice.

THEOREM 2.1. *If $L < 1$, let $\rho_k = \rho(I - \alpha_k A)$ in Algorithm 2.1. Then ρ_k satisfies*

$$\lim_{k \rightarrow \infty} \rho_k = \frac{1 - \mu}{1 + \mu}.$$

Proof. We distinguish two cases depending on the value of L .

Case 1: $L \leq \frac{2}{2-\mu} - \mu$. In this case, it holds that

$$\rho_k \leq 1 - \mu \leq \frac{2}{L + \mu} - 1.$$

Hence, $\alpha_{k+1} = 1 + \rho_k \in (1, \frac{2}{L+\mu}]$ and therefore

$$\rho_{k+1} = \rho(I - \alpha_{k+1} A) = 1 - \mu \alpha_{k+1} = \frac{1 - \mu}{1 + \mu} + \mu \left(\frac{1 - \mu}{1 + \mu} - \rho_k \right).$$

Consequently,

$$\left| \frac{1-\mu}{1+\mu} - \rho_{k+1} \right| = \mu \left| \frac{1-\mu}{1+\mu} - \rho_k \right|.$$

Thus, the sequence ρ_k converges to $\frac{1-\mu}{1+\mu}$ with contraction factor μ .

Case 2: $\frac{2}{2-\mu} - \mu < L < 1$. For $k = 1$, we get $\rho_1 = \rho(I - A) = 1 - \mu$. Whenever $\rho_k > \frac{2}{L+\mu} - 1$, the update rule yields

$$\rho_{k+1} = \rho(I - \alpha_{k+1}A) = L\alpha_{k+1} - 1 = L\rho_k + L - 1 < \rho_k,$$

so the sequence is strictly decreasing. Hence there exists an index $k_0 \geq 1$ such that $\rho_{k_0} \geq \frac{2}{L+\mu} - 1$ and $\rho_{k_0+1} < \frac{2}{L+\mu} - 1$. We now consider two subcases:

Case 2.1: $\rho_{k_0+1} \geq \frac{1-\mu}{1+\mu}$. Using the same relation as in Case 1,

$$\begin{aligned} \rho_{k_0+2} - \frac{1-\mu}{1+\mu} &= \mu \left(\frac{1-\mu}{1+\mu} - \rho_{k_0+1} \right) \\ \rho_{k_0+3} - \frac{1-\mu}{1+\mu} &= \mu^2 \left(\rho_{k_0+1} - \frac{1-\mu}{1+\mu} \right). \end{aligned}$$

This implies $\rho_{k_0+2} \leq \frac{1-\mu}{1+\mu} \leq \rho_{k_0+3} \leq \rho_{k_0+1} < \frac{2}{L+\mu} - 1$. Hence, $\rho_{k_0+i} < \frac{2}{L+\mu} - 1$ and $\alpha_{k_0+i} \in (1, \frac{2}{L+\mu})$ for $i \geq 1$. Following the same procedure as in Case 1, the sequence $\{\rho_k\}$ converges geometrically to $\frac{1-\mu}{1+\mu}$.

Case 2.2: $\rho_{k_0+1} < \frac{1-\mu}{1+\mu}$. Since

$$\rho_{k_0+1} = L\rho_{k_0} + L - 1 \geq L \left(\frac{2}{L+\mu} - 1 \right) + L - 1 = \frac{2L}{L+\mu} - 1,$$

we obtain

$$\rho_{k_0+2} - \frac{1-\mu}{1+\mu} = \mu \left(\frac{1-\mu}{1+\mu} - \rho_{k_0+1} \right) \leq \mu \left(\frac{2}{1+\mu} - \frac{2L}{L+\mu} \right) < \frac{2}{L+\mu} - 1 - \frac{1-\mu}{1+\mu},$$

where the last inequality holds for $L < 1$. Hence $\frac{1-\mu}{1+\mu} < \rho_{k_0+2} < \frac{2}{L+\mu} - 1$, which reduces to **Case 2.1**.

In all cases, the sequence $\{\rho_k\}$ converges to $\frac{1-\mu}{1+\mu}$. □

Remark 2.2. By Theorem 2.1, when $L < 1$, we have

$$\lim_{k \rightarrow \infty} \rho_k = \rho_{\text{GD}}^* + \delta_L,$$

where $\delta_L := \frac{1-\mu}{1+\mu} - \frac{L-\mu}{L+\mu}$ represents the discrepancy introduced by estimating L as 1. As L approaches 1, δ_L approaches 0.

Remark 2.3. In the special case when $L = 1$, if $L \leq \frac{2}{2-\mu} - \mu$, then we have $\mu = 1$, and the adaptive algorithm converges in one iteration. On the other hand, if $L > \frac{2}{2-\mu} - \mu$, it holds that

$$\rho_{k+1} = \alpha_{k+1} - 1 = \rho_k = \dots = \rho_1 = 1 - \mu.$$

Hence, in the implementation with $\rho_k = \rho(I - \alpha_k A)$, if we observe $\rho_2 = \rho_1$, then it implies that $L = 1$ and $\mu = 1 - \rho_1$. We therefore can directly set $\alpha_k = \frac{2}{L+\mu} = \frac{2}{2-\rho_1}$ in Algorithm 2.1.

Computing the spectral radius $\rho_k = \rho(I - \alpha_k A)$ can be computationally expensive, especially for large-scale problems. Therefore, in our implementation, we approximate ρ_k using the geometric average of the ratios of successive residual norms

$$(2.2) \quad \rho_k^l = \begin{cases} \left(\frac{\|\mathbf{r}_k\|}{\|\mathbf{r}_0\|} \right)^{\frac{1}{k}}, & k < l \\ \left(\prod_{i=k-l+1}^k \frac{\|\mathbf{r}_i\|}{\|\mathbf{r}_{i-1}\|} \right)^{\frac{1}{l}}, & k \geq l. \end{cases}$$

If $l = 1$, the above equation simplifies to

$$\rho_k^1 = \frac{\|\mathbf{r}_k\|}{\|\mathbf{r}_{k-1}\|}.$$

If $l = k$, it becomes

$$\rho_k^k = \left(\frac{\|\mathbf{r}_k\|}{\|\mathbf{r}_0\|} \right)^{\frac{1}{k}}.$$

Based on (2.2), we show that Algorithm 2.1 achieves a faster convergence rate than GD with fixed step size $\alpha = 1$.

LEMMA 2.4. *Let ρ_k^l denote the geometric mean of the ratios of successive residual norms, as defined in (2.2). Then, the convergence rate of Algorithm 2.1 satisfies*

$$0 \leq \frac{\|\mathbf{r}_k\|}{\|\mathbf{r}_{k-1}\|} \leq 1 - \mu.$$

Proof. When $k = 1$, with $\alpha_1 = 1$, we have $0 \leq \rho_1^l = \frac{\|\mathbf{r}_1\|}{\|\mathbf{r}_0\|} \leq \|I - A\| = 1 - \mu$.

Case 1: If $l = 1$, assume $0 \leq \rho_k^1 \leq 1 - \mu$ for $k = 2, \dots$, then the step size at each iteration is given by $\alpha_{k+1} = \frac{2}{1 + \rho_k} = 1 + \rho_k$. Thus, one arrives at $1 \leq \alpha_{k+1} \leq 2 - \mu$ and

$$\begin{aligned} \rho_{k+1}^1 &= \frac{\|\mathbf{r}_{k+1}\|}{\|\mathbf{r}_k\|} \leq \|I - \alpha_{k+1} A\| = \max\{|1 - \alpha_{k+1}\mu|, |1 - \alpha_{k+1}L|\} \\ &\leq \max\{1 - \mu, (2 - \mu)L - 1\} = 1 - \mu. \end{aligned}$$

Case 2: For $1 < l < k$, suppose that $0 \leq \rho_k^l \leq 1 - \mu$ holds for all $k = 2, \dots, m$, where $m < l - 1$. Then, similarly, we obtain $1 \leq \alpha_{k+1} \leq 2 - \mu$, $\frac{\|\mathbf{r}_{k+1}\|}{\|\mathbf{r}_k\|} \leq 1 - \mu$, and

$$\rho_{k+1}^l = \left(\frac{\|\mathbf{r}_{k+1}\|}{\|\mathbf{r}_0\|} \right)^{\frac{1}{k+1}} \leq 1 - \mu.$$

This further gives $1 \leq \alpha_l \leq 1 - \mu$, $\frac{\|\mathbf{r}_l\|}{\|\mathbf{r}_{l-1}\|} \leq 1 - \mu$, and $\rho_l^l \leq 1 - \mu$. By induction, one obtains that $\frac{\|\mathbf{r}_{k+1}\|}{\|\mathbf{r}_k\|} \leq 1 - \mu$ and $\rho_{k+1}^l \leq 1 - \mu$ for $k \geq l$.

Case 3: If $l = k$, then by the same argument as in **Case 2**, we obtain the desired result. \square

The above lemma implies

$$-\frac{L - \mu}{L + \mu} \leq \frac{\|\mathbf{r}_k\|}{\|\mathbf{r}_{k-1}\|} - \rho_{\text{GD}}^* \leq 1 - \mu - \frac{L - \mu}{L + \mu},$$

which characterizes how the convergence rate of Algorithm 2.1 deviates from the optimal rate ρ_{GD}^* . Next, we consider the special case $l = 1$ in (2.2). This choice is computationally the most economical in practice and provides a clear insight into how the estimate ρ_k relates to the optimal convergence rate ρ_{GD}^* .

THEOREM 2.5. *Let $\rho_k = \frac{\|\mathbf{r}_k\|}{\|\mathbf{r}_{k-1}\|}$. Suppose $\rho_k = \rho_{\text{GD}}^* + \delta_L + \epsilon_k$, where $\delta_L = \frac{1-\mu}{1+\mu} - \frac{L-\mu}{L+\mu}$. Then, it holds that $\rho_{k+1} = \rho_{\text{GD}}^* + \delta_L + \epsilon_{k+1}$ and ϵ_{k+1} can be bounded as follows.*

Case 1: *If $L > \frac{2}{2-\mu} - \mu$, when $\epsilon_k \in (\frac{2}{L+\mu} - \frac{2}{1+\mu}, 1 - \mu - \frac{1-\mu}{1+\mu}]$,*

$$\epsilon_{k+1} \leq L\epsilon_k,$$

and when $\epsilon_k \in (-\frac{1-\mu}{1+\mu}, \frac{2}{L+\mu} - \frac{2}{1+\mu}]$,

$$\epsilon_{k+1} \leq -\mu\epsilon_k.$$

Case 2: *If $L \leq \frac{2}{2-\mu} - \mu$, it becomes $\epsilon_k \in (-\frac{2-\mu}{1+\mu}, \frac{1}{L+\mu} - \frac{2}{1+\mu}]$, and*

$$\epsilon_{k+1} \leq -\mu\epsilon_k.$$

Proof. For $k = 1$, it yields

$$\rho_1 \leq \|I - \alpha_1 A\| = 1 - \mu = \rho_{\text{GD}}^* + \delta_L + \left(1 - \mu - \frac{1-\mu}{1+\mu}\right).$$

Then, there exists some ϵ_1 such that $\rho_1 = \rho_{\text{GD}}^* + \delta_L + \epsilon_1$. Suppose $\rho_k = \rho_{\text{GD}}^* + \delta_L + \epsilon_k$. Observing that

$$\rho_{k+1} = \frac{\|\mathbf{r}_{k+1}\|}{\|\mathbf{r}_k\|} \leq \|I - \alpha_{k+1} A\| = \max\{|1 - \alpha_{k+1}\mu|, |1 - \alpha_{k+1}L|\},$$

we then estimate ρ_{k+1} in different cases:

Case 1: If $L > \frac{2}{2-\mu} - \mu$, direct computation gives $\epsilon_k \in (-\frac{1-\mu}{1+\mu}, 1 - \mu - \frac{1-\mu}{1+\mu}]$. We further consider two different cases.

Case 1.1: If $\epsilon_k \in (\frac{2}{L+\mu} - \frac{2}{1+\mu}, 1 - \mu - \frac{1-\mu}{1+\mu}]$, it follows that $\alpha_{k+1} \in \left(\frac{2}{L+\mu}, 2 - \mu\right]$.

Also, we have the following estimates:

$$\begin{aligned} \rho_{k+1} &\leq L(1 + \rho_k) - 1 = L(1 + \rho_{\text{GD}}^* + \delta_L + \epsilon_k) - 1 \\ &= \rho_{\text{GD}}^* + L\delta_L + L\epsilon_k - (1 - L)(\rho_{\text{GD}}^* + 1) \leq \rho_{\text{GD}}^* + \delta_L + L\epsilon_k. \end{aligned}$$

This gives $\epsilon_{k+1} \leq L\epsilon_k$.

Case 1.2: If $\epsilon_k \in (-\frac{1-\mu}{1+\mu}, \frac{2}{L+\mu} - \frac{2}{1+\mu}]$, we obtain $\alpha_{k+1} \in (1, \frac{2}{L+\mu}]$ and

$$\begin{aligned} \rho_{k+1} &\leq 1 - \mu(1 + \rho_k) = 1 - \mu(1 + \rho_{\text{GD}}^* + \delta_L + \epsilon_k) \\ &= \rho_{\text{GD}}^* - \mu\delta_L - \mu\epsilon_k - (1 + \mu) \left(\rho_{\text{GD}}^* - \frac{1-\mu}{1+\mu} \right) = \rho_{\text{GD}}^* + \delta_L - \mu\epsilon_k. \end{aligned}$$

Hence, we have $\epsilon_{k+1} \leq -\mu\epsilon_k$.

Case 2: If $L \leq \frac{2}{2-\mu} - \mu$, we have $\epsilon_k + \delta_L \in (-\frac{L-\mu}{L+\mu}, \frac{2(1-L)}{L+\mu}]$ and $\alpha_{k+1} \in (1, \frac{2}{L+\mu}]$. Following the similar analysis as in **Case 1.2** above, we obtain that $\rho_{k+1} \leq \rho_{\text{GD}}^* + \delta_L - \mu\epsilon_k$ and, thus, $\epsilon_{k+1} \leq -\mu\epsilon_k$.

Combining all the above cases, we complete the proof. \square

Remark 2.6. Theorem 2.5 shows that the deviation $\rho_k - \rho_{\text{GD}}^*$ consists of two contributions: ϵ_k , which accounts for the error introduced by the adaptive update, and δ_L , which results from the rescaling of A .

When the largest eigenvalue is accurately estimated, the rescaled matrix satisfies $L \approx 1$ and, in particular, $L \geq \frac{2}{2-\mu} - \mu$. In this regime, the upper bound of the sequence $\{\rho_k\}$ decreases as described in **Case 1**. Conversely, if the largest eigenvalue is not estimated with sufficient accuracy, the problem falls into the regime of **Case 2**. In this situation, no lower bound is available for ϵ_{k+1} , and the convergence rate may fluctuate in practice. The numerical experiments in Section 3.1 further illustrate that, when the largest eigenvalue is not estimated accurately enough, the convergence rate of ρ_k still approaches $\frac{1-\mu}{1+\mu}$, but exhibits a noticeable gap with ρ_{GD}^* due to δ_L .

2.2. Adaptive Accelerated Gradient Descent. In this section, we discuss how to extend the idea of adaptive GD to accelerated methods, such as NAG and HB methods.

2.2.1. Adaptive Nesterov Acceleration. Based on the update rule for NAG method, we have

$$\begin{aligned}\mathbf{x}^{k+1} &= \mathbf{x}^k - \alpha \nabla f(\mathbf{x}^k + \beta(\mathbf{x}^k - \mathbf{x}^{k-1})) + \beta(\mathbf{x}^k - \mathbf{x}^{k-1}) \\ &= \mathbf{x}^k - \alpha(A(\mathbf{x}^k + \beta(\mathbf{x}^k - \mathbf{x}^{k-1})) - \mathbf{b}) + \beta(\mathbf{x}^k - \mathbf{x}^{k-1})\end{aligned}$$

Subtracting \mathbf{x}^* from both sides gives

$$\mathbf{x}^{k+1} - \mathbf{x}^* = (1 + \beta)(I - \alpha A)(\mathbf{x}^k - \mathbf{x}^*) - \beta(I - \alpha A)(\mathbf{x}^{k-1} - \mathbf{x}^*).$$

Define

$$M := \begin{pmatrix} (1 + \beta)(I - \alpha A) & -\beta(I - \alpha A) \\ I & 0 \end{pmatrix} \quad \text{and} \quad \mathcal{R}_k := \begin{pmatrix} \mathbf{r}_k \\ \mathbf{r}_{k-1} \end{pmatrix}.$$

Then the residuals for the NAG follow a two-term recurrence:

$$(2.3) \quad \mathcal{R}_{k+1} = M\mathcal{R}_k, \quad \text{for } k \geq 1.$$

Note that with the optimal parameters given in Table 1, we get $\rho_{\text{NAG}}^* = 1 - \frac{\sqrt{\mu}}{\sqrt{L}}$. Solving for the strong convexity parameter yields $\mu = L(1 - \rho_{\text{NAG}}^*)^2$.

Our adaptive NAG method follows the same procedure as NAG but employs different parameters, i.e.,

$$\begin{aligned}\mathbf{y}_k &= \mathbf{x}_k + \beta_{k+1}(\mathbf{x}_k - \mathbf{x}_{k-1}) \\ \mathbf{x}_{k+1} &= \mathbf{y}_k - \alpha_{k+1}(A\mathbf{y}_k - \mathbf{b}),\end{aligned}$$

where the step size α_k and momentum parameter β_k are determined adaptively based on information from the previous iterations. Consequently, the residual of the adaptive NAG satisfies a similar recurrence relation, $\mathcal{R}_{k+1} = M_k\mathcal{R}_k$, where the error propagation matrix M_k is given by

$$M_k = \begin{pmatrix} (1 + \beta_k)(I - \alpha_k A) & -\beta_k(I - \alpha_k A) \\ I & 0 \end{pmatrix}.$$

Let ρ_k be an empirical approximation of ρ_{NAG}^* . Following the same idea of adaptive GD, since $\mu = L(1 - \rho_{\text{NAG}}^*)^2$, we again use $L = 1$ and approximate μ at iteration k as $\mu_k = (1 - \rho_k)^2$. Consequently, α_{k+1} and β_{k+1} are updated as follows:

$$\alpha_{k+1} = 1 \quad \text{and} \quad \beta_{k+1} = \frac{1 - \sqrt{\mu_k}}{1 + \sqrt{\mu_k}} = \frac{\rho_k}{2 - \rho_k}.$$

The adaptive NAG is summarized in Algorithm 2.2

Algorithm 2.2 Adaptive Nesterov Accelerated Gradient

- 1: **Input:** SPD matrix $A \in \mathbb{R}^{n \times n}$, vector $\mathbf{b} \in \mathbb{R}^n$, initial point $\mathbf{x}_0 \in \mathbb{R}^n$
- 2: **Initialize:** Compute $\mathbf{r}_0 = \mathbf{b} - A\mathbf{x}_0$,
- 3: Perform first step using GD: $\alpha_1 = 1$, $\mathbf{x}_1 = \mathbf{x}_0 - \alpha_1 \nabla f(\mathbf{x}_0)$
- 4: $\mathbf{r}_1 = \mathbf{b} - A\mathbf{x}_1$, $\rho_1 = \|\mathbf{r}_1\|/\|\mathbf{r}_0\|$
- 5: **for** $k = 2, 3, \dots$ **do**
- 6: $\alpha_k = 1$
- 7: $\beta_k = \frac{\rho_{k-1}}{2 - \rho_{k-1}}$
- 8: $\mathbf{y}_{k-1} = \mathbf{x}_{k-1} + \beta_k(\mathbf{x}_{k-1} - \mathbf{x}_{k-2})$
- 9: $\mathbf{x}_k = \mathbf{y}_{k-1} - \alpha_k \nabla f(\mathbf{y}_{k-1})$
- 10: $\rho_k \approx \rho_{\text{NAG}}^*$, where ρ_k is an estimate of ρ_{NAG}^*
- 11: **end for**

We first present a lemma showing that, if the estimation ρ_k is obtained by computing the spectral radius of M_k , then the proposed adaptive NAG Algorithm 2.2 always converges faster than GD with $\alpha = 1$.

LEMMA 2.7. *Let $\rho_k = \rho(M_k)$ in Algorithm 2.2. Then, we have*

$$0 \leq \rho_k \leq 1 - \mu.$$

Proof. Given that the solution at the first step is updated using the GD with $\alpha_0 = 1$, it naturally yields $\rho_1 \leq 1 - \mu$. We now turn to the case when $k \geq 2$. Since A is SPD, it admits an eigenvalue decomposition $A = U\Lambda U^\top$, where U is orthogonal and $\Lambda = \text{diag}(\lambda_1, \dots, \lambda_n)$. By applying a suitable reordering of the coordinates, $M_k \in \mathbb{R}^{2n \times 2n}$ can be transformed into a block-diagonal form with 2×2 diagonal blocks, i.e.,

$$B_k = \text{diag}(B_k^1, B_k^2, \dots, B_k^n), \text{ where } B_k^i = \begin{pmatrix} (1 + \beta_k)(1 - \lambda_i) & -\beta_k(1 - \lambda_i) \\ 1 & 0 \end{pmatrix}.$$

Therefore, ρ_k equals the maximum spectral radius of B_k^i over all i . The eigenvalues of B_k^i can be obtained by solving its characteristic polynomial:

$$(2.4) \quad \theta^2 - (1 + \beta_k)(1 - \lambda_i)\theta + \beta_k(1 - \lambda_i) = 0.$$

When $\beta_k \geq \frac{1 - \sqrt{\lambda_i}}{1 + \sqrt{\lambda_i}}$, the above characteristic equation has either a repeated real root or a pair of complex conjugate roots, with magnitude $\sqrt{\beta_k(1 - \lambda_i)}$. Recall that

$$\beta_{k+1} = \frac{\rho_k}{2 - \rho_k}, \quad \mu_k = (1 - \rho_k)^2.$$

We now analyze the behavior of β_{k+1} under different ranges of ρ_k .

Case 1: When $\rho_k \in [1 - \sqrt{\mu}, 1 - \mu]$, then $\beta_{k+1} \geq \frac{1 - \sqrt{\mu}}{1 + \sqrt{\mu}}$ and

$$\rho_{k+1} = \sqrt{\beta_{k+1}(1 - \mu)} = \sqrt{\frac{\rho_k}{2 - \rho_k}(1 - \mu)} \leq \frac{1 - \mu}{\sqrt{1 + \mu}} < 1 - \mu.$$

Case 2: When $\rho_k \in (0, 1 - \sqrt{\mu})$, there exist blocks whose characteristic equation (2.4) admits two distinct real roots for $\lambda_i \neq 1$, where the larger one is given by:

$$\theta(\lambda_i, \beta_{k+1}) = \frac{(1 + \beta_{k+1})(1 - \lambda_i) + \sqrt{(1 + \beta_{k+1})^2(1 - \lambda_i)^2 - 4\beta_{k+1}(1 - \lambda_i)}}{2}.$$

Since the discriminant $(1 + \beta_{k+1})^2(1 - \lambda_i)^2 - 4\beta_{k+1}(1 - \lambda_i) > 0$ for $\lambda_i \neq 1$, it follows that $(1 + \beta_{k+1})^2(1 - \lambda_i) > 4\beta_{k+1} > 2\beta_{k+1}$. Differentiating θ with respect to λ_i , we obtain

$$\frac{d\theta}{d\lambda_i} = -\frac{1 + \beta_{k+1}}{2} + \frac{-(1 + \beta_{k+1})^2(1 - \lambda_i) + 2\beta_{k+1}}{2\sqrt{(1 + \beta_{k+1})^2(1 - \lambda_i)^2 - 4\beta_{k+1}(1 - \lambda_i)}} < 0.$$

Hence, $\theta(\lambda_i, \beta_{k+1})$ is a decreasing function with respect to λ_i . Similarly, differentiating θ with respect to β_{k+1} , we obtain

$$\begin{aligned} \frac{d\theta}{d\beta_{k+1}} &= \frac{1 - \lambda_i}{2} + \frac{(1 - \lambda_i)^2(1 + \beta_{k+1}) - 2(1 - \lambda_i)}{2\sqrt{(1 + \beta_{k+1})^2(1 - \lambda_i)^2 - 4\beta_{k+1}(1 - \lambda_i)}} \\ &= \frac{(1 - \lambda_i)(\sqrt{(1 + \beta_{k+1})^2(1 - \lambda_i)^2 - 4\beta_{k+1}(1 - \lambda_i)} + (1 - \lambda_i)(1 + \beta_{k+1}) - 2)}{2\sqrt{(1 + \beta_{k+1})^2(1 - \lambda_i)^2 - 4\beta_{k+1}(1 - \lambda_i)}}. \end{aligned}$$

A straightforward computation shows that

$$\begin{aligned} &\sqrt{(1 + \beta_{k+1})^2(1 - \lambda_i)^2 - 4\beta_{k+1}(1 - \lambda_i)} + (1 - \lambda_i)(1 + \beta_{k+1}) - 2 \\ &= \sqrt{(1 + \beta_{k+1})^2(1 - \lambda_i)^2 - 4(1 + \beta_{k+1})(1 - \lambda_i) + 4(1 - \lambda_i)} + (1 - \lambda_i)(1 + \beta_{k+1}) - 2 \\ &< \sqrt{(1 + \beta_{k+1})^2(1 - \lambda_i)^2 - 4(1 + \beta_{k+1})(1 - \lambda_i) + 4} + (1 - \lambda_i)(1 + \beta_{k+1}) - 2 \\ &= 0. \end{aligned}$$

This leads to $\frac{d\theta}{d\beta_{k+1}} < 0$. Since $\theta(\lambda_i, \beta_{k+1})$ is strictly decreasing with respect to both λ_i and β_{k+1} for all $\lambda_i < 1$, we can bound ρ_{k+1} as

$$\rho_{k+1} \leq \max\{\theta(\lambda_i, \beta_{k+1}), \theta(1, \beta_{k+1})\} < \max\{\theta(\mu, 0), 0\} = 1 - \mu.$$

This completes the proof. \square

Next, we further show that ρ_k converges to $1 - \sqrt{\mu}$, which is the optimal convergence rate of standard NAG with $L = 1$, demonstrating Algorithm 2.2 can achieve acceleration.

THEOREM 2.8. *Suppose that $\rho_k = \rho(M_k)$ in Algorithm 2.2. It follows that*

$$\lim_{k \rightarrow \infty} \rho_k = 1 - \sqrt{\mu}.$$

Proof. For $k = 1$, it holds that $0 \leq \rho_1 \leq 1 - \mu$.

We first consider the case when $\rho_1 \in [1 - \sqrt{\mu}, 1 - \mu]$. In this case, we have $\beta_2 \geq \frac{1 - \sqrt{\mu}}{1 + \sqrt{\mu}}$. A brief analysis reveals that

$$\rho_{k+1} = \sqrt{\beta_k(1 - \mu)} = \sqrt{\frac{\rho_k}{2 - \rho_k}(1 - \mu)}$$

is an increasing function with respect to ρ_k on the interval $(0, 1]$. This implies that if $\rho_1 \leq 1 - \mu$, then $\rho_2 \leq \frac{1-\mu}{\sqrt{1+\mu}}$, and more generally, $\rho_k \in [1 - \sqrt{\mu}, 1 - \mu]$ for all $k \geq 2$. We can further show the sequence $\{\rho_k\}$ is nonincreasing: $\rho_{k+1} \leq \rho_k$. By contradiction, suppose $\rho_{k+1} > \rho_k$. Then, we have

$$\rho_{k+1}^2 = \frac{\rho_k}{2 - \rho_k} (1 - \mu) > \rho_k^2 \implies \frac{1 - \mu}{2 - \rho_k} > \rho_k.$$

Rearranging terms leads to $\mu < (1 - \rho_k)^2$, which directly contradicts with $\rho_k \geq 1 - \sqrt{\mu}$. Consequently, the sequence $\{\rho_k\}$ is monotonically decreasing and bounded below. By the Monotone Convergence Theorem, the sequence converges to a finite limit $\hat{\rho}$. At the limit, the fixed-point equation must hold:

$$\hat{\rho} = \sqrt{\frac{\hat{\rho}}{2 - \hat{\rho}} (1 - \mu)}.$$

Solving for $\hat{\rho}$ yields $\lim_{k \rightarrow \infty} \rho_k = \hat{\rho} = 1 - \sqrt{\mu}$.

On the other hand, when $\rho_1 \in (0, 1 - \sqrt{\mu})$, then by invoking Lemma 2.7, one finds that $\frac{d\theta}{d\rho_k} = \frac{d\theta}{d\beta_k} \frac{d\beta_k}{d\rho_k} < 0$, which implies that $\rho_2 \in (1 - \sqrt{\mu}, 1 - \mu)$. A similar argument as the case above yields $\rho_k \in [1 - \sqrt{\mu}, 1 - \mu]$ for $k \geq 2$. Consequently, ρ_k converges to $1 - \sqrt{\mu}$, which completes the proof. \square

Remark 2.9. Theorem 2.8 establishes that ρ_k approaches the convergence factor $1 - \sqrt{\mu}$ corresponding to NAG with $\alpha = 1$ and $\beta = \frac{1-\sqrt{\mu}}{1+\sqrt{\mu}}$. Similar to the GD case, we can rewrite it as

$$\lim_{k \rightarrow \infty} \rho_k = 1 - \sqrt{\mu} = \rho_{\text{NAG}}^* + \left(\frac{\sqrt{\mu}}{\sqrt{L}} - \sqrt{\mu} \right),$$

where the second term $\left(\frac{\sqrt{\mu}}{\sqrt{L}} - \sqrt{\mu} \right)$ represents the discrepancy introduced by estimating L as 1 (cf. Remark 2.2).

We now consider the case $L = 1$. Assume $\rho_k := \rho_{\text{NAG}}^* + \epsilon_k$. When, $\epsilon_k \in [0, \sqrt{\mu} - \mu]$, then $\beta_{k+1} \geq \frac{1-\sqrt{\mu}}{1+\sqrt{\mu}}$. With $\mu = (1 - \rho_{\text{NAG}}^*)^2$, we further have

$$\begin{aligned} \rho_{k+1} &= \sqrt{\beta_{k+1}(1 - \mu)} \\ &= \sqrt{\left(\frac{\rho_{\text{NAG}}^* + \epsilon_k}{2 - \rho_{\text{NAG}}^* - \epsilon_k} \right) (1 - (1 - \rho_{\text{NAG}}^*)^2)} \\ &= \sqrt{\left(\rho_{\text{NAG}}^* + \frac{\epsilon_k}{2 - \rho_{\text{NAG}}^* - \epsilon_k} \right)^2 - \left(\frac{\epsilon_k}{2 - \rho_{\text{NAG}}^* - \epsilon_k} \right)^2} \\ &\leq \rho_{\text{NAG}}^* + \frac{\epsilon_k}{2 - \rho_{\text{NAG}}^* - \epsilon_k} \\ &\leq \rho_{\text{NAG}}^* + \frac{1}{1 + \mu} \epsilon_k. \end{aligned}$$

It follows that $\epsilon_{k+1} \leq \frac{1}{1+\mu} \epsilon_k$. Then, ϵ_k is a monotone and bounded sequence that converges to 0 at a linear rate with factor $\frac{1}{1+\mu}$. This implies that the upper bound of ρ_{k+1} approaches to ρ_{NAG}^* .

As in the adaptive GD case, for practical computation, we approximate ρ_{NAG}^* by ρ_k computed from the geometric average of the ratios of successive residual norms

$$(2.5) \quad \rho_k^l = \begin{cases} \left(\frac{\|\mathcal{R}_k\|}{\|\mathcal{R}_0\|} \right)^{\frac{1}{k}}, & k < l \\ \left(\prod_{i=k-l+1}^k \frac{\|\mathcal{R}_i\|}{\|\mathcal{R}_{i-1}\|} \right)^{\frac{1}{l}}, & k \geq l. \end{cases}$$

For $k \geq l$, we obtain

$$\rho_k^l \leq \left(\prod_{i=k-l+1}^k \|M_i\| \right)^{\frac{1}{l}}.$$

For a general matrix M , the spectral radius is always bounded above by the matrix 2-norm, i.e., $\rho(M) \leq \|M\|$. A sharp characterization of the convergence behavior via the matrix 2-norm is nontrivial, and we defer a rigorous treatment for future work. Nonetheless, the numerical results presented in Section 3 support the effectiveness of Algorithm 2.2 when employing the approximated ρ_k as defined in (2.5).

Remark 2.10. The proposed framework offers broader insights for construction of adaptive variants for a variety of momentum-based algorithms, including the Heavy-Ball (HB) method, HNAG+ [8], the Accelerated Over-Relaxation HB method [39], the Triple Momentum Method [37], C^2 -Momentum [38], and the Information-Theoretic Exact Method [36]). In these methods, the optimal parameters can be expressed in terms of the convergence factor. To illustrate this adaptability, we present an adaptive variant of the HB method, detailed in Algorithm 2.3. For practical implementation, we estimate the optimal convergence rate ρ_{HB}^* by computing the geometric average of the ratios of successive residual norms, as described in (2.5).

Algorithm 2.3 Adaptive Heavy Ball Method

- 1: **Input:** SPD matrix $A \in \mathbb{R}^{n \times n}$, vector $\mathbf{b} \in \mathbb{R}^n$, initial point $\mathbf{x}_0 \in \mathbb{R}^n$
- 2: **Initialize:** Compute $\mathbf{r}_0 = \mathbf{b} - A\mathbf{x}_0$
- 3: Update the first step using GD: $\alpha_1 = 1$, $\mathbf{x}_1 = \mathbf{x}_0 - \alpha_1 \nabla f(\mathbf{x}_0)$
- 4: $\mathbf{r}_1 = A\mathbf{x}_1 - \mathbf{b}$, $\rho_1 = \|\mathbf{r}_1\|/\|\mathbf{r}_0\|$
- 5: **for** $k = 2, 3, \dots$ **do**
- 6: $\alpha_k = (1 + \rho_{k-1})^2$
- 7: $\beta_k = \rho_{k-1}^2$
- 8: $\mathbf{x}_k = \mathbf{x}_{k-1} - \alpha_k \nabla f(\mathbf{x}_{k-1}) + \beta_k (\mathbf{x}_{k-1} - \mathbf{x}_{k-2})$
- 9: $\rho_k \approx \rho_{\text{HB}}^*$, where ρ_k is an estimate of ρ_{HB}^*
- 10: **end for**

3. Numerical Experiments. In this section, we present numerical results to evaluate the performance of the proposed adaptive GD, NAG, and HB methods. We compare these adaptive variants against their standard counterparts configured with theoretically optimal parameters. Notably, various approaches can be used to approximate ρ^* , with the main idea being to approximate the spectral radius of the underlying iteration matrix using observable and computationally inexpensive quantities. In the following experiments, we consider the adaptive strategies described in (2.2) and (2.5) to update parameters dynamically.

3.1. Quadratic optimization problem. We consider solving quadratic optimization problems with diagonal matrix A that have varying eigenvalue distributions. First, to examine the behavior described in Theorem 2.5, we construct diagonal matrices whose eigenvalues are randomly distributed. We sample $\mu \sim \mathcal{U}(0.2, 0.4)$, where $\mathcal{U}(a, b)$ denotes the uniform distribution over the interval $[a, b]$. We consider two cases:

$$L_1 = \frac{1}{2} \left(1 + \frac{2}{2 - \mu} - \mu \right), \quad L_2 = \frac{1}{2} \left(\mu + \frac{2}{2 - \mu} - \mu \right).$$

By construction, $L_1 > \frac{2}{2 - \mu}$, whereas L_2 fails to meet this condition, corresponding to **Cases 1** and **2** in Theorem 2.5, respectively. Given μ and $L = L_j$, $j = 1, 2$, the eigenvalues are generated uniformly in $[\mu, L]$ with the smallest and largest fixed, i.e.,

$$\lambda_1 = \mu, \quad \lambda_n = L_j, \quad \lambda_i \in \mu + (L_j - \mu) \mathcal{U}(0, 1), \quad 2 \leq i \leq n - 1, \quad j = 1, 2.$$

Let $n = 1000$. The vector \mathbf{b} is set to the zero vector. As a result, the quadratic

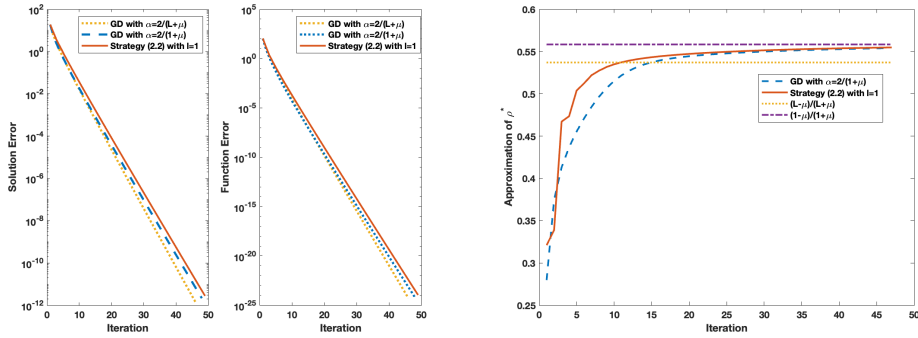


FIG. 1. Error (left) and estimated ρ^* (right) for GD on a diagonal matrix with random eigenvalue distribution satisfying $L > \frac{2}{2 - \mu} - \mu$.

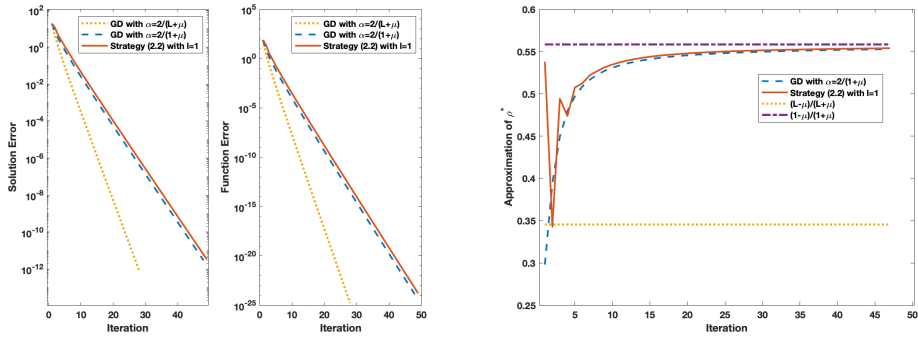


FIG. 2. Error (left) and estimated ρ^* (right) for GD on a diagonal matrix with random eigenvalue distribution satisfying $L \leq \frac{2}{2 - \mu} - \mu$.

optimization problem f attains its minimum at $\mathbf{x}^* = \mathbf{0}$. All methods are initialized with a random vector $\mathbf{x}_0 \in \mathbb{R}^n$ generated by `rand(n, 1)`. The iteration is terminated when either iteration count reaches a maximum `maxIt`, or the gradient norm $\|\nabla f(\mathbf{x}_k)\|$

is less than a tolerance tol . Unless otherwise specified, we use $\text{maxIt} = 3000$ and $\text{tol} = 10^{-12}$. In addition, we define the solution error as $\|\mathbf{x}_k - \mathbf{x}^*\|$, and the function error as $f(\mathbf{x}_k) - f(\mathbf{x}^*)$.

The behavior of the error and approximation of ρ_{GD}^* across the iterations k for two cases are shown in Figure 1 and 2. For comparison, we also plot the results of GD with $\alpha = \frac{1-\mu}{1+\mu}$, where the evolution of ρ_k is characterized by $\|\mathbf{r}_k\|/\|\mathbf{r}_{k-1}\|$. The results are consistent with the observation made in Theorem 2.6. In both cases, ρ_k converges to $\frac{1-\mu}{1+\mu}$, which is the convergence factor of GD with step size $\alpha = \frac{2}{1+\mu}$, rather than the optimal rate ρ_{GD}^* . In particular, larger deviations of L from 1, corresponding to poor rescaling of the Hessian in general cases, result in a convergence factor that is increasingly farther from the optimal one.

Next, we study three methods employing adaptive strategies described in (2.2) and (2.5), with $l = 1, 5$, and k , respectively. The diagonal Hessians are constructed as follows.

Uniform: the eigenvalues are evenly spaced in the interval $[1, 1000]$; that is,

$$\lambda_i \in \text{linspace}(1, 1000, n).$$

Log: the eigenvalues are logarithmically spaced from 1 to 10^5 , representing a wide dynamic range; that is,

$$\lambda_i \in \text{logspace}(0, 5, n).$$

Cluster: 90% of the eigenvalues are sampled uniformly in the narrow range $[0, 0.1]$, while the remaining 10% are outliers centered around 0.7; that is,

$$\lambda_{\text{cluster}} \sim \mathcal{U}(0, 0.1), \quad \lambda_{\text{outlier}} \sim \mathcal{U}(0.65, 0.75), \quad \text{then} \quad \lambda_i \in \{\lambda_{\text{cluster}}, \lambda_{\text{outlier}}\}.$$

Assuming that a more accurate estimate of the largest eigenvalue λ_n is available, we can rescale the matrix A such that $L = 1$. Here, for standard methods, we use strategy (2.2) and (2.5) with $l = 1$ to estimate ρ_k at each iteration. Besides, for NAG and HB, we initialize the first iteration using a single GD step with fixed step size $\alpha_0 = 1$: $\mathbf{x}_1 = \mathbf{x}_0 - \alpha_0 \nabla f(\mathbf{x}_0)$.

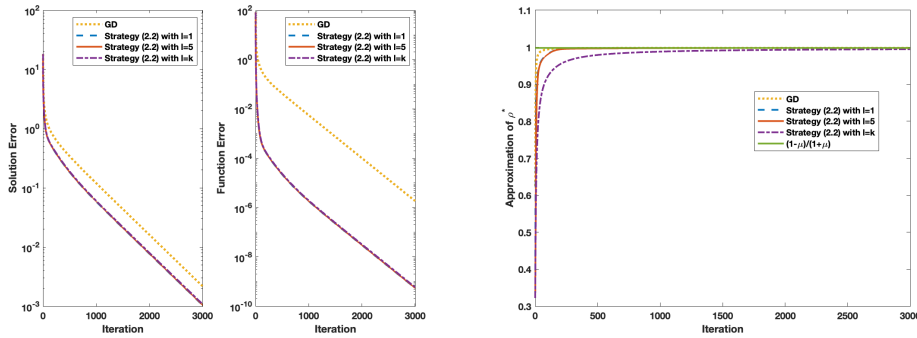


FIG. 3. Error (left) and estimated ρ^* (right) for GD on a diagonal matrix with uniform eigenvalue distribution ($n = 1000$).

Figure 3-5 report the performance of GD and its adaptive variants (strategy (2.2) with $l = 1, 5$, and k) on diagonal matrices with varying eigenvalue distributions. We see that for all tests, the estimated ρ_k approaches ρ_{GD}^* from below. In both the

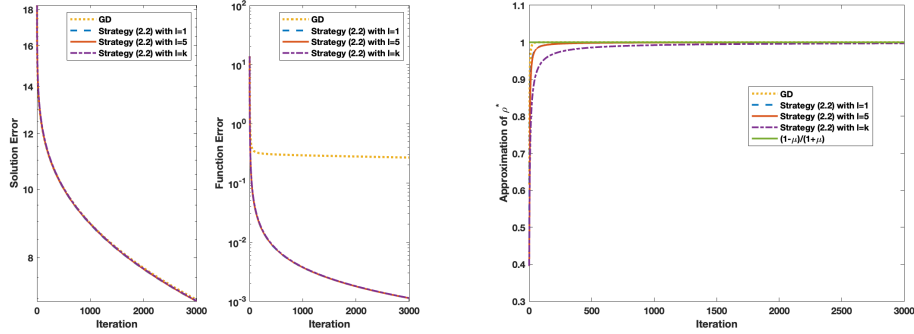


FIG. 4. Error (left) and estimated ρ^* (right) for GD on a diagonal matrix with log-spaced eigenvalue distribution ($n = 1000$).

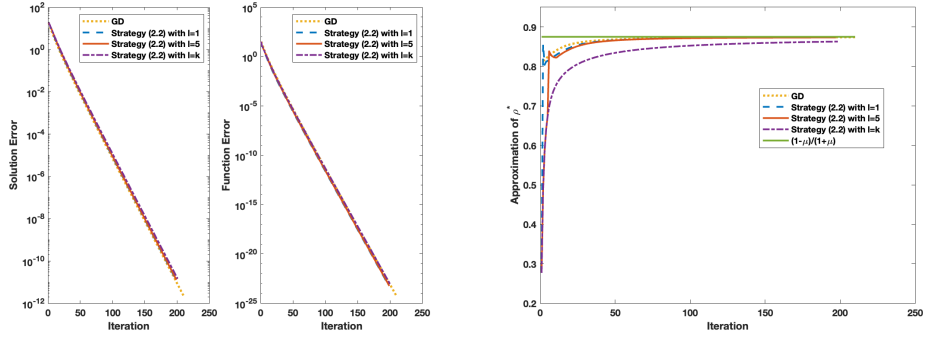


FIG. 5. Error (left) and estimated ρ^* (right) for GD on a diagonal matrix with clustered eigenvalue distribution ($n = 1000$).

uniform and log-spaced cases, the adaptive variants exhibit higher accuracy, reducing the function value error by several orders of magnitude compared to standard GD. This is because the eigenvalues are relatively dispersed. Consequently, even when two iterates are close in the ℓ^2 norm, their function values may differ significantly. In the clustered setting, the performance of the adaptive variants is comparable to that of standard GD. Furthermore, strategy (2.2) with $l = k$, yields a smoother approximation of ρ_k , as it averages over all previous iterations.

The comparison of NAG and its adaptive variants (strategy (2.5) with $l = 1, 5$, and k) are summarized in Figure 6-8. We notice that strategy (2.5) with $l = 1$ and 5 produce results that are comparable to standard NAG, demonstrating the effectiveness of the adaptive strategies. While strategy (2.5) with $l = k$ tends to perform slightly worse in the uniform and log-spaced cases. This is due to the fact that, in this case, ρ_k incorporating the entire history of iterations, leads to a more conservative choice. Moreover, the estimated convergence bound ρ_k shows oscillations, but eventually converges to ρ_{NAG}^* . This behavior results from using only the most recent iteration, and hence the estimate is sensitive to short-term fluctuations.

The results of HB and the corresponding adaptive variants across various eigenvalue distributions are described in Figure 9-11. Under the same number of iterations, both strategy (2.5) with $l = 1$ and 5 achieve higher accuracy than the standard HB

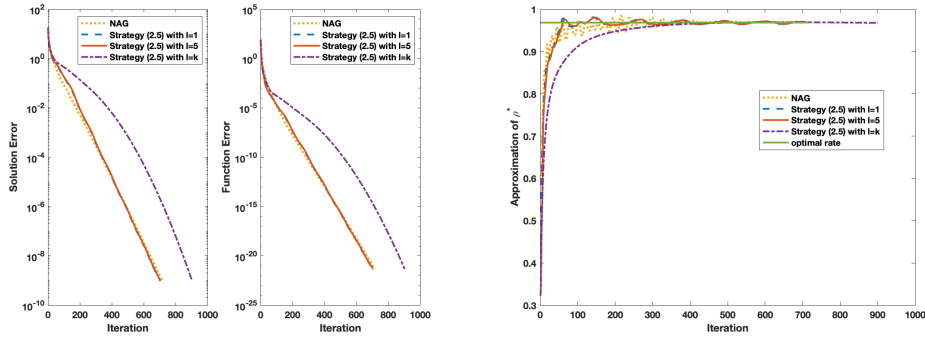


FIG. 6. Error (left) and estimated ρ^* (right) for NAG on a diagonal matrix with uniform eigenvalue distribution ($n = 1000$).

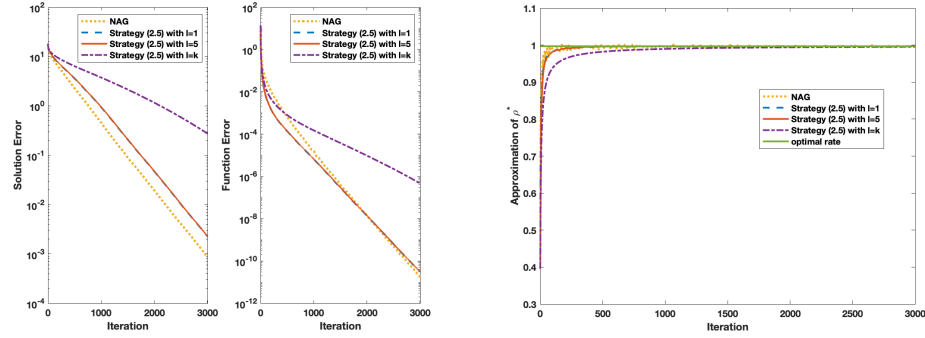


FIG. 7. Error (left) and estimated ρ^* (right) for NAG on a diagonal matrix with log-spaced eigenvalue distribution ($n = 1000$).

method for the uniform and log-spaced cases. Notably, for these two cases, the standard HB, as it is sensitive to parameter choices, shows some oscillation at the early stage. As shown in the clustered case, while strategy (2.5) with $l = 1$ achieves higher accuracy, its estimation of ρ_{HB}^* shows greater oscillations. Generally, strategy (2.5) with $l = 5$ maintains both accuracy and stability, making it the most balanced choice among the HB variants.

3.2. Logistic regression problem with regularization. Logistic regression is a fundamental statistical method used for binary classification, with wide range applications in fields such as finance [4, 14], medical [42, 31], and marketing [10, 5]. Consider a dataset consists of p samples, each characterized by n features. The feature matrix $A \in \mathbb{R}^{n \times p}$ is constructed such that each column represents a distinct sample. For each sample i , the response is binary, taking values $b_i \in \{-1, 1\}$. We define the vector of all labels as $\mathbf{b} = [b_1, b_2, \dots, b_p]^T$. Logistic regression models the conditional probability of the label b_i given the input $A_{:,i}$ (the i -th column of A) via:

$$P(b_i | A_{:,i}) = \text{sigm}(b_i(\mathbf{x}^T A_{:,i})).$$

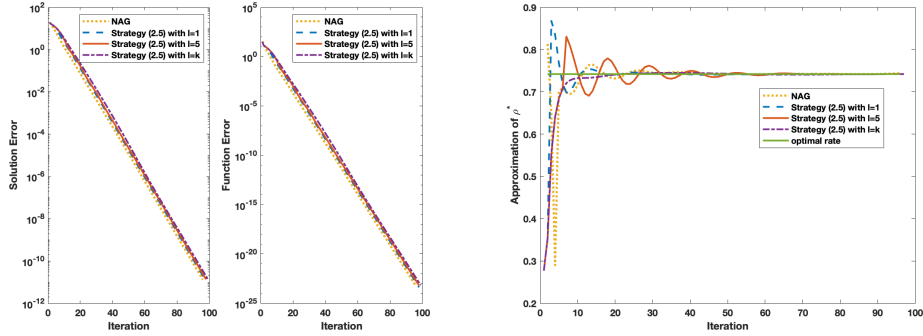


FIG. 8. Error (left) and estimated ρ^* (right) for NAG on a diagonal matrix with clustered eigenvalue distribution ($n = 1000$).

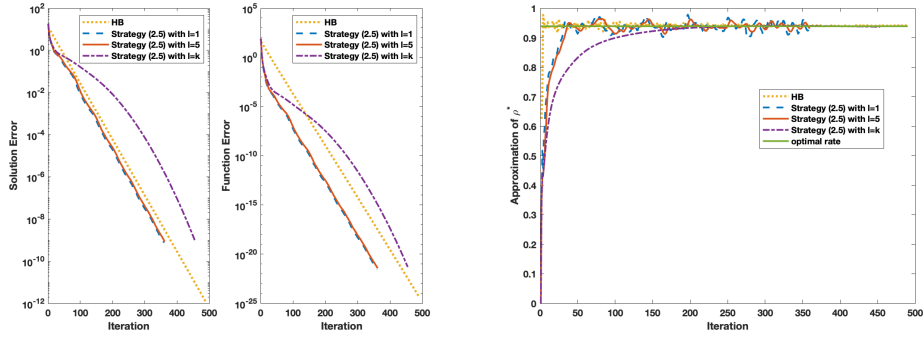


FIG. 9. Error (left) and estimated ρ^* (right) for HB on a diagonal matrix with uniform eigenvalue distribution ($n = 1000$).

Here the sigmoid function is $\text{sigm}(z) := \frac{1}{1+e^{-z}}$. To estimate the weight vector $\mathbf{x} \in \mathbb{R}^n$, we consider minimizing the negative log-likelihood:

$$f(\mathbf{x}) = \frac{\xi}{2} \mathbf{x}^T \mathbf{x} + \sum_{i=1}^p \log(1 + e^{-b_i(\mathbf{x}^T A_{:,i})}),$$

where ξ is the regularization parameter, ensuring that the optimization problem is strongly convex and preventing overfitting. The gradient and Hessian for $f(\mathbf{x})$ are given by:

$$\begin{aligned} \nabla f(\mathbf{x}) &= \xi \mathbf{x} + \sum_{i=1}^p \frac{e^{-b_i(\mathbf{x}^T A_{:,i})}}{1 + e^{-b_i(\mathbf{x}^T A_{:,i})}} (-b_i A_{:,i}) \\ \nabla^2 f(\mathbf{x}) &= \xi I + \sum_{i=1}^p \text{sigm}(b_i(\mathbf{x}^T A_{:,i})) (1 - \text{sigm}(b_i(\mathbf{x}^T A_{:,i}))) A_{:,i} A_{:,i}^T. \end{aligned}$$

Note that $0 < \text{sigm}(z)(1 - \text{sigm}(z)) \leq \frac{1}{4}$, so the eigenvalues of the Hessian matrix lie in the range $[\xi, \xi + \frac{1}{4}\lambda_{\max}(AA^T)]$. This motivates us to approximate the minimum eigenvalue and the maximum eigenvalue of the Hessian by $\tilde{\mu} = \xi$ and $\tilde{L} = \xi + \frac{1}{4}\|AA^T\|_1$,

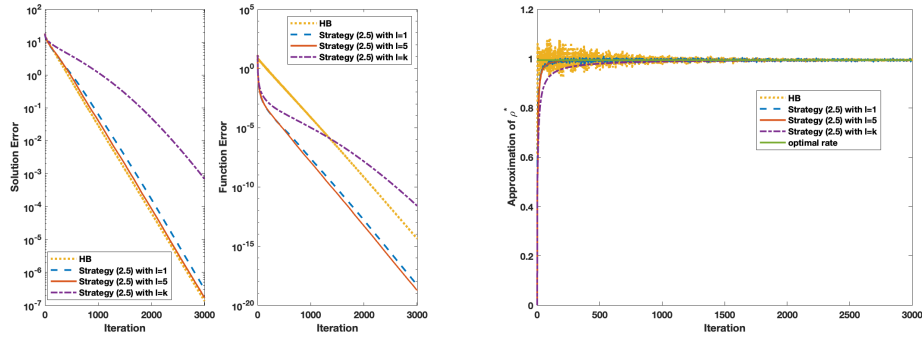


FIG. 10. Error (left) and estimated ρ^* (right) for HB on a diagonal matrix with log-spaced eigenvalue distribution ($n = 1000$).

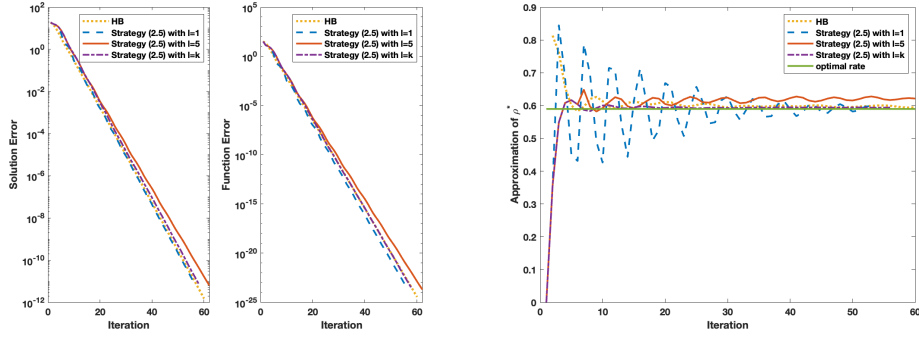


FIG. 11. Error (left) and estimated ρ^* (right) for HB on a diagonal matrix with clustered eigenvalue distribution ($n = 1000$).

respectively. Thus, the original algorithms apply the fixed $\tilde{\mu}$ and \tilde{L} . For the adaptive method, with \tilde{L} , the update rules are given by:

$$\mu_k = \begin{cases} \frac{1 - \rho_k}{1 + \rho_k} \tilde{L}, & \text{for GD} \\ (1 - \rho_k)^2 \tilde{L}, & \text{for NAG} \\ \left(\frac{1 - \rho_k}{1 + \rho_k}\right)^2 \tilde{L}, & \text{for HB.} \end{cases}$$

In addition, for both NAG and HB, the first iteration is a GD step with a step size of $\alpha = \frac{2}{\tilde{\mu} + \tilde{L}}$.

In this test, we focus on the classical setting where $p > n$, often arising when data are abundant. Here, $A \in \mathbb{R}^{n \times p}$ is generated with entries sampled from the standard normal distribution, and the binary label vector $\mathbf{b} \in \{-1, 1\}^p$ is drawn from a Bernoulli distribution with $0 \mapsto -1$. We use $n = 500$, $p = 2000$, $\xi = 0.1$ and $\mathbf{x}_0 = \mathbf{0}$. The stopping criterion for all tested algorithms is either a maximum of `maxIt` or iterations or a relative gradient norm $\|\nabla f(\mathbf{x}_k)\|/\|\nabla f(\mathbf{x}_0)\| < \text{tol}$ with `maxIt` = 350 and `tol` = 10^{-6} . To get a reference solution \mathbf{x}_{ref} , we employ the NAG for convex objectives [33] with a higher precision (`maxIt` = 10^5 , `tol` = 10^{-12}). The performance is then evaluated using the solution error $\|\mathbf{x}_k - \mathbf{x}_{\text{ref}}\|$, and the function error $f(\mathbf{x}_k) - f(\mathbf{x}_{\text{ref}})$.

In Figure 12–14, we show the results of GD, NAG, and HB and their adaptive variants. Since the optimal rate bound ρ^* changes at each iteration, we estimate it dynamically for standard methods using the strategy (2.2) and (2.5) with $l = 1$, respectively. We observe that for GD, the adaptive strategies achieve similar results to that of the original method with fixed \tilde{L} and $\tilde{\mu}$ in both accuracy and iteration count. For NAG, strategy (2.5) with $l = k$ performs the worst. In contrast, strategy (2.5) with $l = 1$ and 5 achieve accuracy of the same order of magnitude as NAG with fixed \tilde{L} and $\tilde{\mu}$ but using fewer iterations. This is because adaptive algorithms dynamically adapt to local curvature information of the objective. On the other hand, here NAG only relies on fixed parameters derived from $\tilde{\mu}$ and \tilde{L} , which can be poor estimations. A similar phenomenon is observed for HB, where adaptive variants show better results than the standard one.

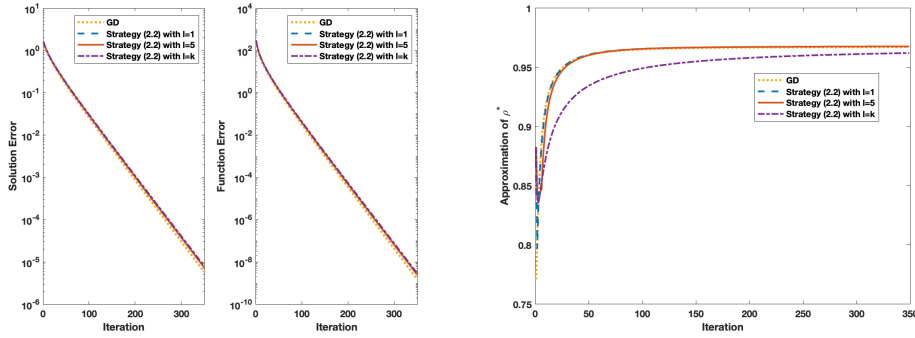


FIG. 12. Error (left) and estimated ρ^* (right) for GD and its variants on the logistic regression problem.

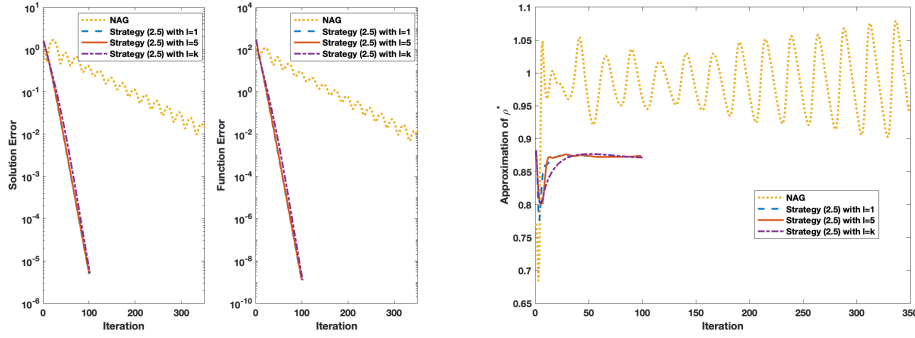


FIG. 13. Error (left) and estimated ρ^* (right) for NAG and its variants on the logistic regression problem.

To further examine whether the observed behavior arises from inaccurate parameter choices or from the effectiveness of the adaptive algorithms, we use power iteration to estimate L , and in the original methods we use L with shifted power iteration (with tolerance 10^{-6} and max 500 iterations) to estimate μ at each iteration. Then we arrive at the following results, as shown in Figure 15–17. We observe that the adaptive algorithms and the original methods with estimated L and μ exhibit

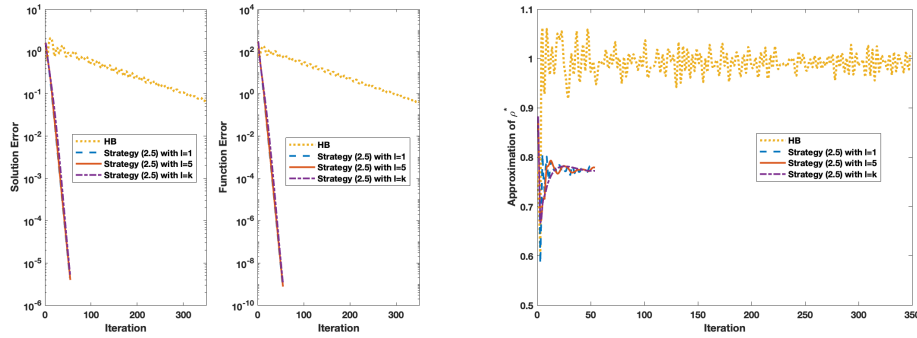


FIG. 14. Error (left) and estimated ρ^* (right) for HB and its variants on the logistic regression problem.

similar performance. Compared to the previous tests with fixed \tilde{L} and $\tilde{\mu}$, fewer iterations are required. Nonetheless, as mentioned, estimating L at each step increases the computational cost.

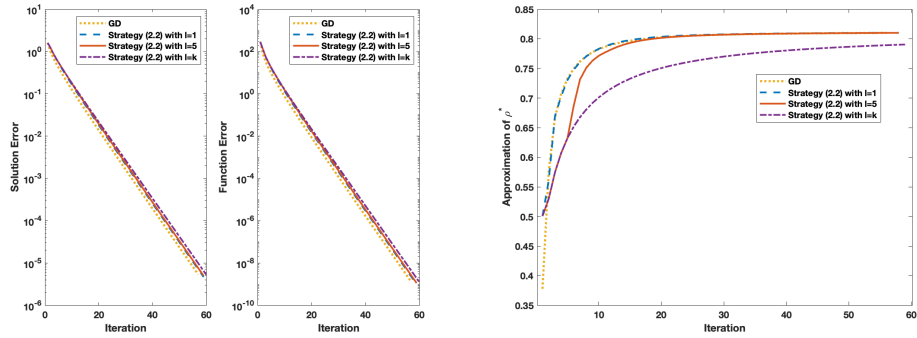


FIG. 15. Error (left) and estimated ρ^* (right) for GD and its variants on the logistic regression problem.

3.3. Huber-TV regularized image denoising. Total Variation (TV) regularization [30] has been widely used in image processing [6, 32, 18]. The key idea is to promote piecewise constant images while preserving sharp edges. The classical TV model penalizes the L^1 norm of the image gradient, which leads to the undesirable staircasing effect [25]. To address this, a common strategy is replacing the non-smooth TV term with a Huber smoothing function:

$$h_\delta(t) = \begin{cases} \frac{t^2}{2\delta}, & \text{for } |t| \leq \delta, \\ |t| - \frac{\delta}{2}, & \text{for } |t| > \delta, \end{cases}$$

where $\delta > 0$. Then, the Huber-TV regularization is defined as $\int_{\Omega} h_\delta(|\nabla u(x)|) dx$. This regularizer is often employed in image denoising [7]. In this setting, one arrives

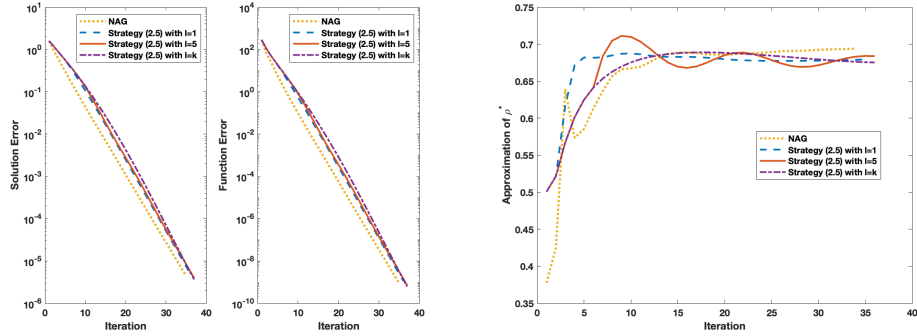


FIG. 16. Error (left) and estimated ρ^* (right) for NAG and its variants on the logistic regression problem.

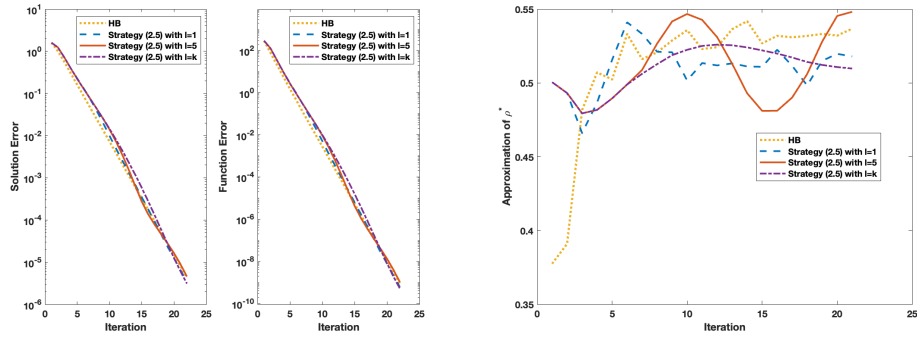


FIG. 17. Error (left) and estimated ρ^* (right) for HB and its variants on the logistic regression problem.

at the following Huber-TV denoising model:

$$\min_{u:\Omega \rightarrow \mathbb{R}} f(u) = \frac{\xi}{2} \int_{\Omega} (u(x) - u_0(x))^2 dx + \eta \int_{\Omega} h_{\delta}(|\nabla u(x)|) dx,$$

where $u_0 \in \mathbb{R}^{n \times m}$ is a given noisy image corrupted by Gaussian noise, $\xi > 0$ is the fidelity parameter, $\eta > 0$ controls smoothness, and $|\nabla u(x)| = \sqrt{u_x(x)^2 + u_y(x)^2}$. Then, the gradient of the objective can be written as

$$\nabla f(u) = \xi(u - u_0) - \eta \operatorname{div} \left(h'_{\delta}(|\nabla u|) \frac{\nabla u}{|\nabla u|} \right),$$

For any $v \in H^1(\Omega)$, the Hessian of f at u applied to v is given by

$$\nabla^2 f(u)[v] = \xi v - \eta \operatorname{div} (\mathcal{A}(u) \nabla v),$$

where $\mathcal{A}(u)$ is defined as

$$\mathcal{A}(u) = \begin{cases} \frac{1}{\delta} I, & |\nabla u| \leq \delta, \\ \frac{1}{|\nabla u|} \left(I - \frac{\nabla u \nabla u^T}{|\nabla u|^2} \right), & |\nabla u| > \delta. \end{cases}$$

Noting that when $|\nabla u| > \delta$, $I - \frac{\nabla u \nabla u^\top}{|\nabla u|^2}$ is an orthogonal projector and, therefore, its 2-norm equals 1. Consequently, we have

$$\left\| \frac{1}{|\nabla u|} \left(I - \frac{\nabla u \nabla u^\top}{|\nabla u|^2} \right) \right\| \leq \frac{1}{|\nabla u|} \leq \frac{1}{\delta}.$$

Hence, $\mathcal{A}(u)$ is uniformly bounded in the matrix 2-norm by $1/\delta$.

In the following tests, we consider an image $u_0 \in \mathbb{R}^{256 \times 256}$ corrupted by Gaussian noise with zero mean and variance 0.05^2 . We set $\xi = 4$, $\eta = 0.06$ and $\delta = 0.05$. The gradient ∇u is approximated using forward finite differences, with Neumann boundary conditions. Thus the induced discrete Laplacian operator satisfies $\|\Delta\|_1 \leq 8$. Combining the above bounds, the strong convexity constant and the Lipschitz constant are estimated as $\tilde{\mu} = \xi$, $\tilde{L} = \xi + \frac{8\eta}{\delta}$, respectively.

The results are summarized in Figure 18-20. We observe that the adaptive GD algorithms with strategy (2.2) require a similar number of iterations as GD with fixed \tilde{L} and $\tilde{\mu}$ to achieve comparable objective decrease. This is because the estimated L and μ remain close to the actual values across iterations. Moreover, the convergence factors ρ^k for the adaptive algorithms are close to the one for GD with fixed parameters. Similar results can also be observed for the adaptive NAG algorithms. For the HB method, using fixed parameters leads to fewer iterations under the same objective decrease. We also observe that, for the method with fixed parameters, the estimated convergence factor ρ_k gradually approaches $(\tilde{L} - \tilde{\mu})/(\tilde{L} + \tilde{\mu})$. However, for the adaptive algorithms, ρ_k stabilizes around 0.7. This behavior may result from the difference in initialization: the adaptive algorithms start with GD using step size $1/\tilde{L}$, while the fixed-parameter approach initializes GD with step size $1/(\tilde{L} + \tilde{\mu})$. This difference is further amplified by the parameter sensitivity of the HB method.

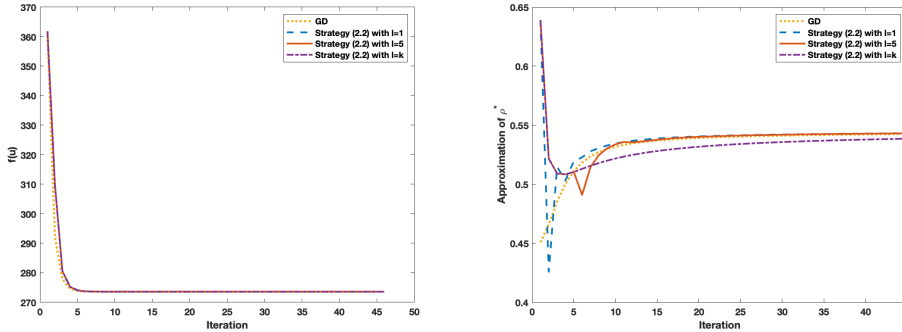


FIG. 18. Decay of the objective value (left) and estimated ρ^* (right) for GD and its variants on the image denoising problem.

4. Conclusion. By utilizing the ratio of residual norms at two consecutive iterations as an empirical estimate of the upper bounds on convergence rates, we propose an adaptive framework for tuning the step size and momentum parameters in first-order methods for unconstrained quadratic optimization problems. We establish that the sequence of iterates generated by these adaptive gradient methods converges to \mathbf{x}^* at a rate at least as favorable as that of GD with a step size of $1/L$.

Numerical results on both quadratic and general strongly convex optimization problems demonstrate the effectiveness of our proposed methods, showing that the

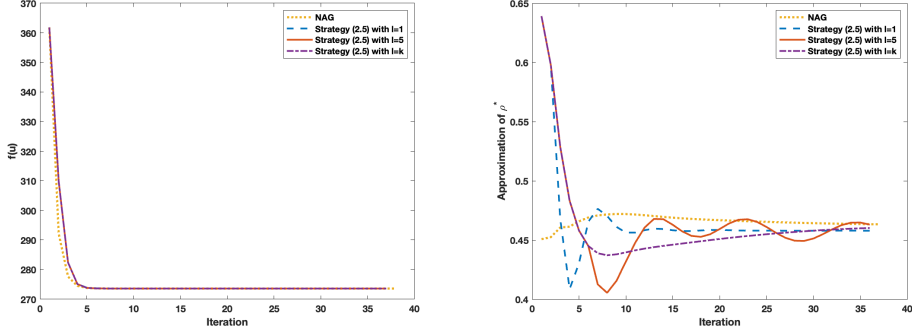


FIG. 19. Decay of the objective value (left) and estimated ρ^* (right) for NAG and its variants on the image denoising problem.

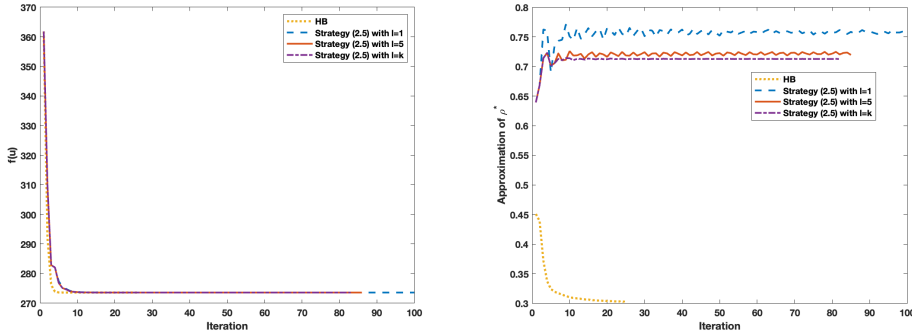


FIG. 20. Decay of the objective value (left) and estimated ρ^* (right) for HB and its variants on the image denoising problem.

adaptive algorithms achieve efficiency comparable to their accelerated counterparts with optimal parameters. However, as noted, a gap remains between the spectral radius and the matrix 2-norm in our current analysis. To bridge this gap, a potential direction for future research involves utilizing Lyapunov functions [41, 40] to construct adaptive algorithms and provide the corresponding theoretical analysis.

Acknowledgments. The authors wish to thank James H. Adler for many insightful and helpful discussions and suggestions.

REFERENCES

- [1] L. ARMJO, *Minimization of functions having lipschitz continuous first partial derivatives*, Pacific Journal of mathematics, 16 (1966), pp. 1–3.
- [2] C. AUSTIN, S. POLLOCK, AND Y. ZHU, *Dynamically accelerating the power iteration with momentum*, Numerical Linear Algebra with Applications, 31 (2024), p. e2584.
- [3] L. BOTTOU, F. E. CURTIS, AND J. NOCEDAL, *Optimization methods for large-scale machine learning*, SIAM review, 60 (2018), pp. 223–311.
- [4] D. BROBY, *The use of predictive analytics in finance*, The Journal of Finance and Data Science, 8 (2022), pp. 145–161.
- [5] M. BURINSKIENE AND V. RUDZKIENE, *Application of logit regression models for the identification of market segments*, Journal of Business Economics and Management, 8 (2007), pp. 253–258.

- [6] A. CHAMBOLLE, *An algorithm for total variation minimization and applications*, Journal of Mathematical imaging and vision, 20 (2004), pp. 89–97.
- [7] A. CHAMBOLLE AND T. POCK, *An introduction to continuous optimization for imaging*, Acta Numerica, 25 (2016), pp. 161–319.
- [8] L. CHEN AND Z. XU, *Hnag++: A super-fast accelerated gradient method for strongly convex optimization*, arXiv preprint arXiv:2510.16680, (2025).
- [9] E. K. CHONG, W.-S. LU, AND S. H. ZAK, *An Introduction to Optimization: With Applications to Machine Learning*, John Wiley & Sons, 2023.
- [10] C. CONSTANTIN, *Using the logistic regression model in supporting decisions of establishing marketing strategies*, Bulletin of the Transilvania University of Brasov. Series V: Economic Sciences, (2015), pp. 43–50.
- [11] A. D’ASPREMONT, D. SCIEUR, A. TAYLOR, ET AL., *Acceleration methods*, Foundations and Trends® in Optimization, 5 (2021), pp. 1–245.
- [12] A. A. GOLDSTEIN, *Cauchy’s method of minimization*, Numerische Mathematik, 4 (1962), pp. 146–150.
- [13] B. GOUJAUD, A. TAYLOR, AND A. DIEULEVEUT, *Provable non-accelerations of the heavy-ball method: B. goujaud et al.*, Mathematical Programming, (2025), pp. 1–59.
- [14] M. HASAN, T. LE, AND A. HOQUE, *How does financial literacy impact on inclusive finance?*, Financial innovation, 7 (2021), p. 40.
- [15] M. ITO AND M. FUKUDA, *Nearly optimal first-order methods for convex optimization under gradient norm measure: An adaptive regularization approach*, Journal of Optimization Theory and Applications, 188 (2021), pp. 770–804.
- [16] L. LESSARD, B. RECHT, AND A. PACKARD, *Analysis and design of optimization algorithms via integral quadratic constraints*, SIAM Journal on Optimization, 26 (2016), pp. 57–95.
- [17] G. LI AND T. K. PONG, *Calculus of the exponent of kurdyka–łojasiewicz inequality and its applications to linear convergence of first-order methods*, Foundations of computational mathematics, 18 (2018), pp. 1199–1232.
- [18] M. LUSTIG, D. DONOHO, AND J. M. PAULY, *Sparse mri: The application of compressed sensing for rapid mr imaging*, Magnetic Resonance in Medicine: An Official Journal of the International Society for Magnetic Resonance in Medicine, 58 (2007), pp. 1182–1195.
- [19] Y. MALITSKY AND K. MISHCHENKO, *Adaptive gradient descent without descent*, arXiv preprint arXiv:1910.09529, (2019).
- [20] Y. MALITSKY AND K. MISHCHENKO, *Adaptive proximal gradient method for convex optimization*, Advances in Neural Information Processing Systems, 37 (2024), pp. 100670–100697.
- [21] J. MATTINGLEY AND S. BOYD, *Real-time convex optimization in signal processing*, IEEE Signal processing magazine, 27 (2010), pp. 50–61.
- [22] D. MEIGNAN, S. KNUST, J.-M. FRAYRET, G. PESANT, AND N. GAUD, *A review and taxonomy of interactive optimization methods in operations research*, ACM Transactions on Interactive Intelligent Systems (TiiS), 5 (2015), pp. 1–43.
- [23] Y. NESTEROV, *Gradient methods for minimizing composite functions*, Mathematical programming, 140 (2013), pp. 125–161.
- [24] Y. E. NESTEROV, *A method for solving a convex programming problem with convergence rate $O(1/k^2)$* , Soviet Mathematics Doklady, 269 (1983), pp. 372–376.
- [25] M. NIKOLOVA, *Minimizers of cost-functions involving nonsmooth data-fidelity terms. application to the processing of outliers*, SIAM Journal on Numerical Analysis, 40 (2002), pp. 965–994.
- [26] B. O’DONOGHUE AND E. CANDES, *Adaptive restart for accelerated gradient schemes*, Foundations of computational mathematics, 15 (2015), pp. 715–732.
- [27] D. P. PALOMAR AND Y. C. ELDAR, *Convex optimization in signal processing and communications*, Cambridge university press, 2010.
- [28] R. L. RARDIN, *Optimization in operations research*, vol. 166, Prentice Hall Upper Saddle River, NJ, 1998.
- [29] V. ROULET AND A. D’ASPREMONT, *Sharpness, restart and acceleration*, Advances in Neural Information Processing Systems, 30 (2017).
- [30] L. I. RUDIN, S. OSHER, AND E. FATEMI, *Nonlinear total variation based noise removal algorithms*, Physica D: nonlinear phenomena, 60 (1992), pp. 259–268.
- [31] P. SCHOBER AND T. R. VETTER, *Logistic regression in medical research*, Anesthesia & Analgesia, 132 (2021), pp. 365–366.
- [32] E. Y. SIDKY AND X. PAN, *Image reconstruction in circular cone-beam computed tomography by constrained, total-variation minimization*, Physics in Medicine & Biology, 53 (2008), p. 4777.
- [33] W. SU, S. BOYD, AND E. J. CANDES, *A differential equation for modeling nesterov’s accelerated*

gradient method: Theory and insights, Journal of Machine Learning Research, 17 (2016), pp. 1–43.

[34] J. J. SUH AND S. MA, *An adaptive and parameter-free nesterov's accelerated gradient method for convex optimization*, arXiv preprint arXiv:2505.11670, (2025).

[35] S. SUN, Z. CAO, H. ZHU, AND J. ZHAO, *A survey of optimization methods from a machine learning perspective*, IEEE transactions on cybernetics, 50 (2019), pp. 3668–3681.

[36] A. TAYLOR AND Y. DRORI, *An optimal gradient method for smooth strongly convex minimization*, Mathematical Programming, 199 (2023), pp. 557–594.

[37] B. VAN SCOY, R. A. FREEMAN, AND K. M. LYNCH, *The fastest known globally convergent first-order method for minimizing strongly convex functions*, IEEE Control Systems Letters, 2 (2017), pp. 49–54.

[38] B. VAN SCOY AND L. LESSARD, *The fastest known first-order method for minimizing twice continuously differentiable smooth strongly convex functions*, IEEE Control Systems Letters, (2025).

[39] J. WEI AND L. CHEN, *Accelerated over-relaxation heavy-ball method: Achieving global accelerated convergence with broad generalization*, 2025.

[40] A. WIBISONO, A. C. WILSON, AND M. I. JORDAN, *A variational perspective on accelerated methods in optimization*, proceedings of the National Academy of Sciences, 113 (2016), pp. E7351–E7358.

[41] A. C. WILSON, B. RECHT, AND M. I. JORDAN, *A lyapunov analysis of accelerated methods in optimization*, Journal of Machine Learning Research, 22 (2021), pp. 1–34.

[42] E. C. ZABOR, C. A. REDDY, R. D. TENDULKAR, AND S. PATIL, *Logistic regression in clinical studies*, International Journal of Radiation Oncology* Biology* Physics, 112 (2022), pp. 271–277.